10th IFAC Symposium on Robot Control
International Federation of Automatic Control
September 5-7, 2012. Dubrovnik, Croatia

Modeling of a Three Wheeled Omnidirectional Robot Including Friction Models

Mariane Dourado Correia, André Gustavo Scolari Conceição

Department of Electrical Engineering, Polytechnical School,
Federal University of Bahia, Salvador, Brasil
(e-mail: [marianedc,andre.gustavo]@ufba.br).

Abstract: This paper presents a model of a three-wheeled omnidirectional robot including a static friction model. Besides the modeling is presented a practical approach in order to estimate the coefficients of coulomb and viscous friction, which used sensory information about force and velocity of the robot's center of mass. The proposed model model has the voltages of the motors as inputs and the linear and angular velocities of the robot as outputs. Actual results and simulation with the estimated model are compared to demonstrate the performance of the proposed modeling.

Keywords: Models, Friction, Parameter estimation, Autonomous mobile robots.

1. INTRODUCTION

The robotic platforms resulting from attaching omnidirectional wheels to a chassis are called holonomic because, the resulting vehicle can drive a path with independent orientation and X-Y motion or the controllable degrees of freedom is equal to the total degrees of freedom then the robot. Omnidirectional wheels roll forward like normal wheels, but slide sideways with no friction (or very little friction). This differs from a traditional Ackerman-steered vehicle or a tracked vehicle that must use skid-steering.

An omnidirectional robot is able to perform movements in any direction without the need to reorient, allowing more mobility and increasing the robot's degree of freedom. This feature is achieved by controlling the omnidirectional wheels, combining their vectorial forces and velocities (Conceicao et al., 2009). For a dynamic and kinematic model of the robot, it is necessary to consider magnitudes like speed, acceleration and strength that is provided by the actuators, whereas the energy put into the system discussed in (C.C. de Wit and Bastin, 1997).

From the studies on the dynamics and kinematics involved in the movement of the omnidirectional robot, it is possible to develop a model that approximates the reality. For the modeling of estimation of coefficients of friction it is necessary to analyze the models of static and dynamic friction. The classical models of friction are composed of different components and aspects of the frictional force. The main idea is that friction opposes its magnitude motion and it is independent of the speed of the contact area (Hess and Soom, 1990). As an example of static model there is Coulumb's friction model, usually combined with viscous friction model for a better fit of the experimental data, see ((Baril, 1993); (Friedland and Park, 1992)). The Karnopp model is used to detect zero speed (Karnopp, 1985).

Dynamic models have been of great interest due to advances in hardware that allows the implementation of friction compensators. The Dahl model (Dahl, 1976) was introduced in order to simulate the control systems with friction, see (Astrom, 1998). The Lugre model is presented in (Canudas de Wit et al., 1995) and its analysis and modeling are made by the elastic bristles found in (Olsson, 1996), known to be popular in the time domain, and its control and simulation friction are due to its simplicity and integration of pre-slip and slip systems.

This paper presents a dynamic model of an omnidirectional mobile robot that considers the coulomb and viscous friction in the composition of forces of the robot's center of mass. To estimate the coefficients of friction, an experimental method that uses sensory information of force and velocity of the robot's center of mass is used. This method, proposed in (Conceicao et al., 2009) for a four-wheeled robot, is now tested in a three-omnidirectional-wheeled robot. An analysis of model behavior in different operating situations, including the dead zone effects, is presented.

The paper is organized as follows. In section 2, the model of an omnidirectional-wheeled robot is presented and a state space representation is proposed. Section 3 presents a parameters estimation of the friction coefficients of the model. In section 4, current results achieved by the model are discussed, addressing the advantages and disadvantages. The final considerations are presented in section 5.

2. MODELING

2.1 Kinematics of the robot

By geometric parameters of the robot and the robot's body frame, in Figure 1(a), the motion equations are as follows:

$$\dot{\xi} = R^T(\theta)\dot{\xi_r} \tag{1}$$

where an orthogonal rotation matrix $R(\theta)$ is defined to map the world frame into the robot frame, and vice versa:

$$R(\theta) = \begin{bmatrix} cos(\theta) & sin(\theta) & 0 \\ -sin(\theta) & cos(\theta) & 0 \\ 0 & 0 & 1 \end{bmatrix} \quad (2)$$

The robot pose is fully described by the vector: $\xi = [x_r \quad y_r \quad \theta]^T$, where x_r and y_r is the localization of the point P in the world frame, and θ the angular difference between the world and robot frames. $\dot{\xi}_r = [v \;\; v_n \;\; w]^T$ is the velocity vector at the robot frame and describes the linear velocity of the robot at the point P, represented by the orthogonal components v and v_n, and the angular velocity of the robot's body, represented by w.

The relationships between robot velocities (v, v_n and w) and wheel's angular velocities (w_{m_i}, for $i = 1, ..., 3$) are given by:

$$\begin{bmatrix} v \\ v_n \\ w \end{bmatrix} = \begin{bmatrix} 0 & \frac{r_2\sqrt{3}}{3} & \frac{-r_3\sqrt{3}}{3} \\ \frac{2r_1}{3} & \frac{r_2}{3} & \frac{r_3}{3} \\ \frac{r_1}{3b} & \frac{r_2}{3b} & \frac{r_3}{3b} \end{bmatrix} \begin{bmatrix} w_{m_1} \\ w_{m_2} \\ w_{m_3} \end{bmatrix}, \quad (3)$$

with b the distance between the point P and robot's wheels, r_i the radius of each wheel i, and the angle δ equal to 30 degrees.

2.2 Dynamics of the robot

The omnidirectional mobile robot model is developed based on the dynamics, kinematics and dynamics of DC motors of the robot. By Newton's law of motion and the robot's body frame, in Figure 1(a), the dynamic model is described by

$$F_v(t) - B_v v(t) - C_v sgn(v(t)) = M\frac{dv(t)}{dt}, \quad (4)$$

$$F_{v_n}(t) - B_{v_n} v_n(t) - C_{v_n} sgn(v_n(t)) = M\frac{dv_n(t)}{dt}, \quad (5)$$

$$\Gamma(t) - B_w w(t) - C_w sgn(w(t)) = I_n\frac{dw(t)}{dt}, \quad (6)$$

where,

$$sgn(\alpha) = \begin{cases} 1, & \alpha > 0, \\ 0, & \alpha = 0, \\ -1, & \alpha < 0. \end{cases}$$

$F = [F_v \quad F_{v_n} \quad \Gamma]^T$ represents the vector force (F_v and F_{v_n}) in the robot frame and the moment (Γ) around the center of gravity for the mobile robot (point P). The robot mass is M and the robot inertia moment is I_n. The viscous frictions ($B_v v(t)$, $B_{v_n} v_n(t)$ and $B_w w(t)$) represent a retarding force, which is a linear relationship between the applied force and the velocity. The coulomb frictions ($C_v sgn(v(t))$, $C_{v_n} sgn(v_n(t))$ and $C_w sgn(w(t))$) represent a retarding force that has constant amplitude with respect to the change of velocity, but the sign changes with the reversal of the direction of velocity, (Kuo, 1995). B_v, B_{v_n} and B_w are the viscous friction coefficients related to v, v_n and w respectivelly, and C_v, C_{v_n} and C_w the coulomb friction coefficients.

The relationships between the robot's traction forces and the wheel's traction forces are,

$$F_v(t) = cos(\delta)(f_2(t) - f_3(t)) \quad (7)$$

$$F_{v_n}(t) = -f_1(t) + sen(\delta)f_2(t) + sen(\delta)f_3(t) \quad (8)$$

$$\Gamma(t) = (f_1(t) + f_2(t) + f_3(t))b. \quad (9)$$

The wheel's traction force on each wheel i (for $i = 1, ..., 3$) is

$$f_i(t) = \frac{T_i(t)}{r_i}. \quad (10)$$

with T_i the rotation torque of the wheels.

The dynamics of each DC motor i (for $i = 1, ..., 3$) can be described using the following equations,

$$u_i(t) = L_{a_i}\frac{di_{a_i}(t)}{dt} + R_{a_i} i_{a_i}(t) + K_{v_i} w_{m_i}(t), \quad (11)$$

$$T_i(t) = l_i K_{t_i} i_{a_i}(t), \quad 0 \leq i_{a_i}(t) \leq i_{max} \quad (12)$$

where L_{a_i} are the motor's armature inductance, R_{a_i} are the motor's armature resistance, l_i are the motor's gear ratio reduction, and w_{m_i} the angular velocity of the wheels. The armature current is limited to save battery, where $i_{max}(A)$ is a design parameter. The armature voltage is $u(t)$, with input signal constraints: $-6(Volts) \leq u(t) \leq 6(Volts)$ for $t \geq 0$. In SI unit system, the values of K_t (motor's torque constant) and K_v (motor's electromotive force constant) are identical, see Kuo (1995): $K_t(N.m/A) = K_v(Volts/(rad/sec))$.

2.3 State Space Representation

In this subsection, the robot model in the state-variable form is presented. By combining previously mentioned equations, it is possible to show that model equations can be rearranged into a variation of the state space that can be described as

$$\dot{x}(t) = Ax(t) + Bu(t) + Ksgn(x(t)) \quad (13)$$

$$y(t) = Cx(t) \quad (14)$$

where the vector $u(t) = [u_1(t) \;\; u_2(t) \;\; u_3(t)]^T$ is the input and the vectors $y(t) = x(t) = [v(t) \;\; v_n(t) \;\; w(t)]^T$ are the output and the state-variables of the system. Considering $l = l_{1...3}$, $r = r_{1...3}$, $R_a = R_{a_{1...3}}$ and $K_t = K_{t_{1...3}}$, the simplified state-variable-form matrices defining this system are

$$A = \begin{bmatrix} -\frac{3l^2K_t^2}{2MR_ar^2} - \frac{B_v}{M} & 0 & 0 \\ 0 & -\frac{3l^2K_t^2}{2MR_ar^2} - \frac{B_{v_n}}{M} & 0 \\ 0 & 0 & -\frac{3b^2l^2K_t^2}{JR_ar^2} - \frac{B_w}{I_n} \end{bmatrix},$$

$$B = \frac{lK_t}{R_ar}\begin{bmatrix} 0 & \frac{cos(\delta)}{M} & -\frac{cos(\delta)}{M} \\ \frac{-1}{M} & \frac{sen(\delta)}{M} & \frac{sen(\delta)}{M} \\ \frac{b}{I_n} & \frac{b}{I_n} & \frac{b}{I_n} \end{bmatrix},$$

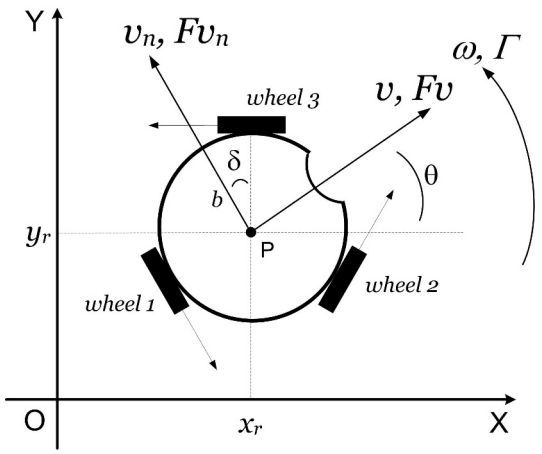

(a) Geometric parameters and reference frames.

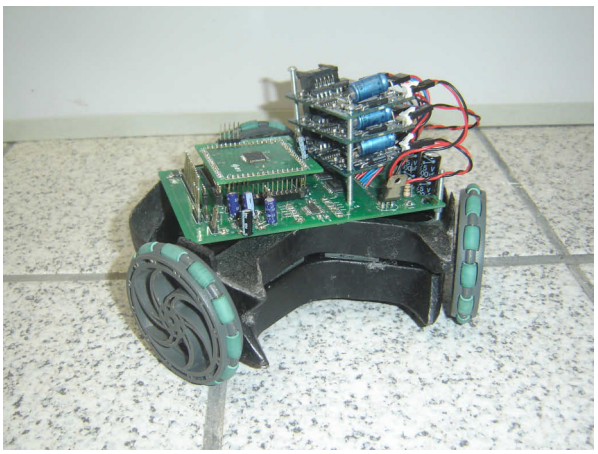

(b) Omnidirectional mobile robot.

Fig. 1. Wheeled Robot.

$$K = \begin{bmatrix} -\frac{C_v}{M} & 0 & 0 \\ 0 & -\frac{C_{v_n}}{M} & 0 \\ 0 & 0 & -\frac{C_\omega}{I_n} \end{bmatrix}, \quad C = I.$$

Analyzing (13), one can observe that the nonlinearity lies in the $Ksgn(x(t))$ term.

3. ESTIMATION OF THE COEFFICIENTS OF FRICTION

The method of estimation consists of applying velocities v, v_n and w in the robot, and measuring the traction forces F_v, F_{v_n} and the torque Γ, with the robot on steady-state velocity. Because of a steady-state velocity (null derivatives) and considering positive velocities, equations (4 - 6) can be simplified:

$$F_v(t) = B_v v(t) + C_v \tag{15}$$

$$F_{vn}(t) = B_{vn} v_n(t) + C_{vn} \tag{16}$$

$$\Gamma(t) = B_w w(t) + C_w \tag{17}$$

In this method, it is possible to estimate the viscous (B_v, B_{vn}, B_w) and coulomb (C_v, C_{vn}, C_w) frictions. Table 1 shows the applied voltages (causing the robot velocities) and the resulting velocities, forces and torques. The forces and the torque can be calculated using the motor's currents, see equations (7-12).

The effects of dead zones of the motors should be considered in conducting the experiments, as reflected in the velocities of the robot's center of mass. Thus, the lowest applied voltages are close to the values on which the mobile base starts moving. For example, the first line of Table 1 shows the voltages u = (0, 1.2, -1.2) applied to the motors but the base is stopped, however for the voltages u = (0, 2, -2) the base is moving. The same happens for vn and w velocities. Figure 2 presents some curves of velocities, and their currents used to obtain the forces. It can be seen in Figure 2(a) that applying the voltage of 3 volts on motor 2 and the voltage of -3 volts on motor 3 generated a velocity of about 0.74 meters per second in the direction of velocity v. The respective currents are shown in Figure 2(a). The same analysis can be made for the other graphs in Figure 2.

u_i $(volts)$	v (m/s)	F_v (N)
0 ;1.2;-1.2	0	2.25
0;2;-2	0.37	2.48
0;3;-3	0.74	2.79
0;4;-4	1.08	3.28
u_i $(volts)$	v_n (m/s)	F_{vn} (N)
-1.5;0.75;0.75	0	1.47
-3;1.5;1.5	0.42	1.97
-4;2;2	0.75	2.33
-5;2.5;2.5	1.08	2.49
u_i $(volts)$	w (rad/s)	Γ $(N.m)$
0.25;0.25;0.25	0	0.10
1.5;1.5;1.5	5.84	0.14
2;2;2	8.04	0.18
2.5;2.5;2.5	10.02	0.21

Table 1. Values of voltages, velocities, forces and torques.

As the values of the velocities and forces are known, the frictions coefficients may be estimated. The least-squares line method was used to approximate the set of data to a linear model (equation of the straight line). Figure 3 shows the applied velocity, resulting force, and the best fitting line. The resulting equations with the estimated coefficients are presented in Table 2. The robot mass was balanced, while for the moment of inertia of the robot was used the moment of inertia of a cylinder with the same mass and dimensions of radius and height of the robot.

	Equations	B_v,B_{vn} B_w	C_v,C_{vn} C_w
v	$F_v(t) = 0.94v(t) + 2.2$	0.94	2.2
v_n	$F_{vn}(t) = 0.96v_n(t) + 1.5$	0.96	1.5
w	$\Gamma(t) = 0.01w(t) + 0.099$	0.01	0.099

Table 2. Equations and coefficients.

Summarizing, the parameters of the motors, geometric parameters and estimated parameters are presented in Table 3.

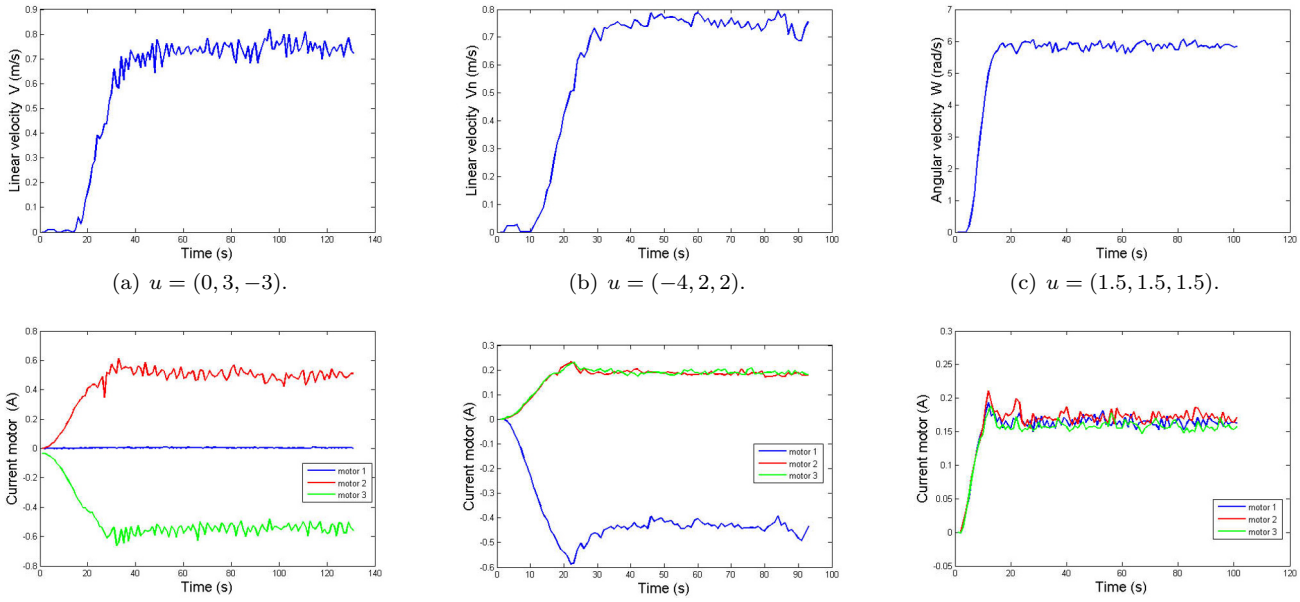

(a) $u = (0, 3, -3)$. (b) $u = (-4, 2, 2)$. (c) $u = (1.5, 1.5, 1.5)$.

(d) $i_{a_1}, i_{a_2}, i_{a_3}$. (e) $i_{a_1}, i_{a_2}, i_{a_3}$. (f) $i_{a_1}, i_{a_2}, i_{a_3}$.

Fig. 2. Velocities and Currents.

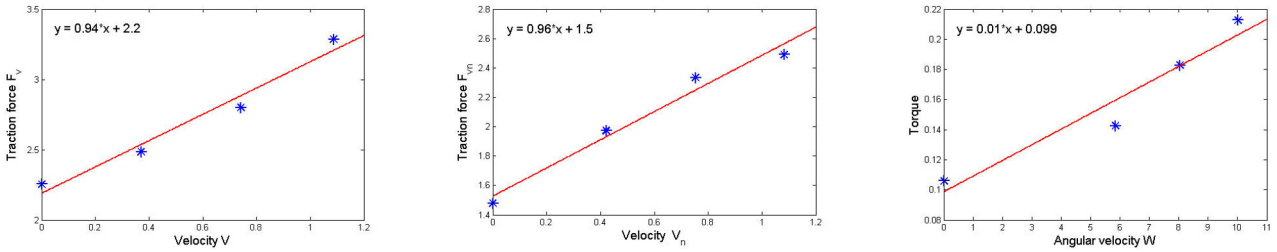

(a) F_v *versus* v. (b) F_{vn} *versus* v_n. (c) Γ *versus* w.

Fig. 3. Relation between forces and torque with velocity.

Table 3. Parameters of the model.

Simbol	*Description*	*Values*
$B_v(N/m/s)$	viscous friction coefficient related to v	0.94
$B_{v_n}(N/m/s)$	viscous friction coefficient related to v_n	0.96
$B_\omega(N/rad/s)$	viscous friction coefficient related to ω	0.01
$C_v(N)$	coulomb friction coefficient related to v	2.2
$C_{v_n}(N)$	coulomb friction coefficient related to v_n	1.5
$C_\omega(N.m)$	coulomb friction coefficient related to ω	0.099
$b(m)$	radius of the robot	0.1
$M(kg)$	mass of the robot	1.5
$I_n(kg.m^2)$	inertia moment of the robot	0.025
δ	angle	30^o
$r_1, r_2, r_3(m)$	radius of the wheels	0.035
l_1, l_2, l_3	reduction of the motors	19:1
$L_{a_{1\ldots3}}(H)$	motor's armature inductance	0.00011
$R_{a_{1\ldots3}}(\Omega)$	motor's armature resistance	1.69
$K_{v_{1\ldots3}}(Volts/rad/s)$	motor's emf constant	0.0059
$K_{t_{1\ldots3}}(N.m/A)$	motor's torque constant	0.0059

4. ANALYSIS OF THE MODEL

This section presents results to verify the behavior of the estimated model and compare it with real results of the robot. The model has the voltage of the motors as inputs and velocity of the robot's center of mass as outputs. Experiments were carried out by applying voltages on motors and in the model, as shown in Table 4. For example, while applying zero volt in motor 1, 2 volts in motor 2 and -2 volts in motor 3, the velocity of the robot is in the direction of vector v.

The results of simulation and the robot velocities are shown in Figure 4. The model gives a good representation of the robot state. For cases in which the robot has velocities v and v_n, the presence of noise is bigger when

compared with the velocities w. This is easily explained by the geometry of the robot, which to generate velocities in the v direction only two of the three motors are active, in addition the wheels have an angle of 30 degrees related to velocity vector v (see Figure 1(b)). In the case of w, the three motors are active simultaneously in the same direction and with the same input voltage, making less noise. It is important to say that, in open loop experiments, any undulation in the floor would cause a small difference in the transient and steady state responses.

The model considers the effect of static friction and therefore the open loop response should represent the dead zone. To verify this effect, experiments were performed as shown in Figure 5. For the velocities v, Figure 5(a), the model represented accurately the effect of dead zone compared with the robot. For velocities w, Figure 5(b), the model also achieved a good performance. For v and v_n the necessary voltages for the robot start to move are bigger (around 1 volt) due to the presence of a larger static friction caused by the geometry of the mobile base. To overcome this inertia in w, the necessary voltage is around 0.3 volts.

Velocity v		
Motor 1 $u_1(volts)$	**Motor 2** $u_2(volts)$	**Motor 3** $u_3(volts)$
0	2	-2
0	3	-3
0	4	-4
Velocity v_n		
Motor 1 $u_1(volts)$	**Motor 2** $u_2(volts)$	**Motor 3** $u_3(volts)$
-2	1	1
-3	1.5	1.5
-4	2	2
Velocity w		
Motor 1 $u_1(volts)$	**Motor 2** $u_2(volts)$	**Motor 3** $u_3(volts)$
2	2	2
3	3	3
4	4	4

Table 4. Applied voltages.

5. CONCLUSION

In this paper, a mobile robot modeling including coulomb and viscous friction in the composition of the robot forces has been proposed. This is a simplified friction model when compared to existing models in the literature (for example, Lugre and Dahl). The model showed a good agreement with real data and with the mapping of the dead zone effects. We can see an acceptable difference between the estimated values, taking into account that the measured values of currents and velocities have a considerable noise, and any irregularity in the floor can cause alterations in parameters of the robot. A practical approach to estimate the coefficients of friction was used, based on sensory information from the motor current and the robot speed, easily applicable in any configuration of vehicle which provides these logs. Finally, a model that represents non-linear elements are essential to controllers design, especially when the robot is subjected to different operating conditions such as uneven terrain or the transportation of different loads, which require maximum forces of the actuators. An example of control application can be seen in Araújo et al. (2011), where a methodology for state feedback MPC (Model Predictive Control) synthesis applied to the trajectory tracking control problem was proposed. In the referred work, the model used in this work was used to predict the future robot positions and orientations and takes into account elements such as saturation and friction.

ACKNOWLEDGEMENTS

The authors would like to acknowledge the financial support of the Brazilian National Research Council - CNPq.

REFERENCES

Astrom, K. J. (1998). Control of systems with friction, *Proceedings of the Fourth International Conference on Motion and Vibration Control*, pp. 25–32.

Baril, C. (1993). *Control od Mechanical Systems Affected by Friction and Other Nondifferentiable Nonlinearities*, Phd thesis, Israel Institute of Techonology, Switzerland.

Barreto, J. C., Conceição, A. S. and Dorea, C. E. T. (2010). Predictive control of an omnidirectional mobile robot with friction compensation, *Latin American Robotics Symposium and Intelligent Robotics Meeting - LARS2010*, pp. 30–35.

Canudas de Wit, C., Olsson, H., Astrom, K. and Lischinsky, P. (1995). A new model for control of systems with friction, *IEEE Transactions on Automatic Control* **40**(3): 419 –425.

C.C. de Wit, B. S. and Bastin, G. (1997). *Theory of Robot Control*, Springer-Verlag Ltd.

Conceicao, A., Moreira, A. and Costa, P. (2009). Practical approach of modeling and parameters estimation for omnidirectional mobile robots, *IEEE/ASME Transactions on Mechatronics* **14**(3): 377 –381.

Dahl, P. R. (1976). Solid friction damping of mechanical vibrations, *AIAA Journal* pp. 1675–1682.

Friedland, B. and Park, Y. J. (1992) On adaptive friction compensation, *IEEE Transactions on Automatic Control* **37**(10): 1609 –1612.

Hess, D. P. and Soom, A. (1990). Friction at a lubricated line contact operating at oscillating sliding velocities, *Journal of Tribology* **112**(1): 147–152.

Karnopp, D. (1985). Computer simulation of stick-slip friction in mechanical dynamic systems, *Journal of Dynamic Systems, Measurement, and Control* **107**(1): 100–103.

Kuo, B. C. (1995). *Automatic Control Systems*, John Wiley & Sons Ltd.

Olsson, H. (1996). *Control Systems with Friction*, Phd thesis, Lund Institute of Technology, University of Lund, Lund.

Araújo, H. X., Conceicao, A. G. S., Oliveira, G. H. C., Pitanga, J. R. (2011). Model Predictive Control Based on LMIs Applied to an Omni-Directional Mobile Robot, *Proceedings of the 18th IFAC World Congress,* **18**(1): 8171–8176.

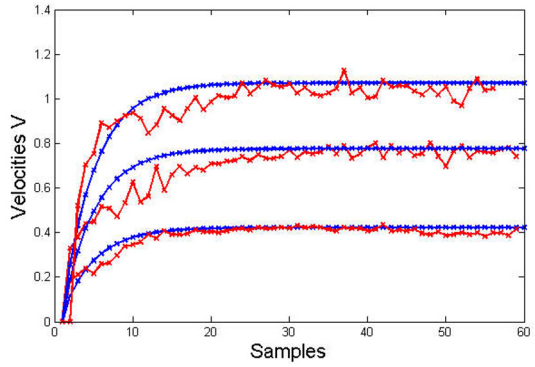

(a) Inputs u: (0; 2;-2), (0; 3; -3) e (0;4; -4).

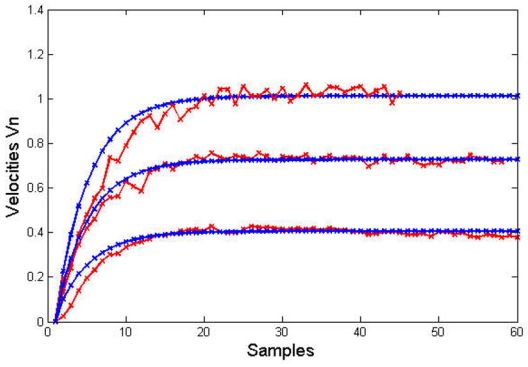

(b) Inputs u: (-2;1;1), (-3;1.5;1.5) e (-4;2;2).

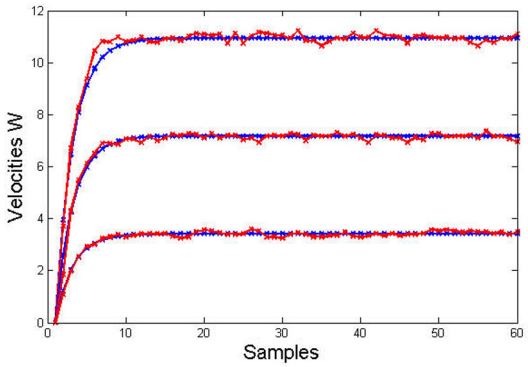

(c) Inputs u: (2;2;2), (3;3;3) e (4;4;4).

Fig. 4. Real and simulation results.

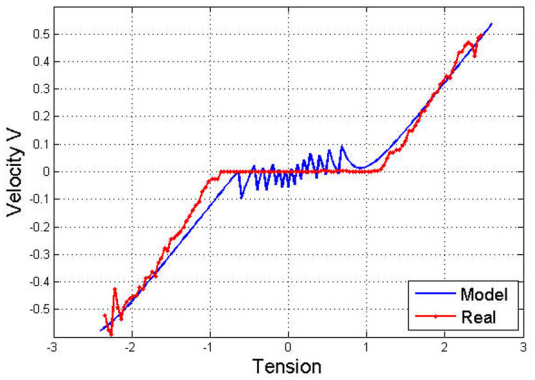

(a) Velocity v.

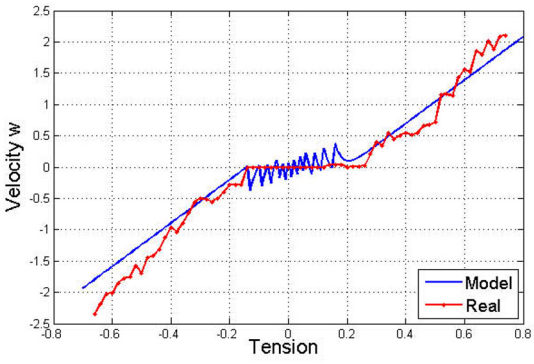

(b) Velocity w.

Fig. 5. Dead-zone effect.